

# **CHAPTER 3**

## **Experimental**

### 3.1 Method of sample preparation

The objective of this experiment is to synthesize lithium transition metal oxide cathode materials for lithium batteries. This research is concentrated on developing a good cathode material with high electrochemical performances. The electrode was prepared using sol-gel method.

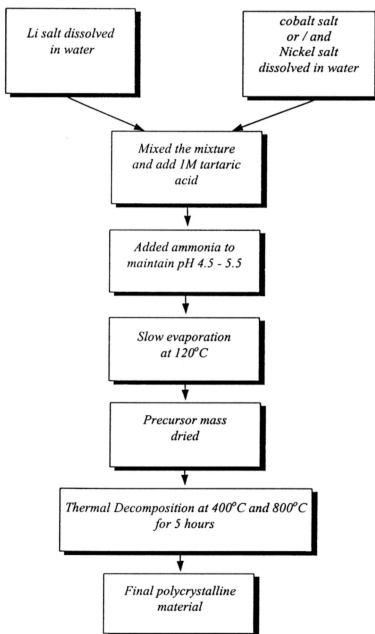


Figure 3.1: Flow chart showing soft-chemistry synthesis of  $\text{LiCo}_x\text{Ni}_{1-x}\text{O}_2$

Table 3.1. Amounts of chemical used

	LiOH.H <sub>2</sub> O	Co(NO <sub>3</sub> ) <sub>2</sub> .6H <sub>2</sub> O	Ni(NO <sub>3</sub> ) <sub>2</sub> .6H <sub>2</sub> O
Sample A	0.1 mole	0.04 mole	0.06 mole
Sample C	0.1 mole	0.02mole	0.08 mole
Sample E	0.1 mole	-	0.1 mole
Sample F	0.1 mole	0.1 mole	-

Lithium cobalt oxide, lithium cobalt nickel oxide and lithium nickel oxide was prepared according to the process schematically illustrated in figure 3.1. A stoichiometric amount of high purity lithium hydroxide, cobalt nitrate and nickel nitrate salts corresponding to a cationic ratio Li:Ni and Co = 1:1 was dissolved in minimum distilled water. An equal amount of tartaric acid of concentration of 1 mol dm<sup>-3</sup> was added slowly to the mixture. A gel was formed due to poor solubility of nickel, cobalt or lithium tartrate. Ammonia solution of concentration 1 mol dm<sup>-3</sup> was added slowly until a pH 4.5 to 5.5 was achieved. The gel was heated at 120°C with continous stirring until the gel turned into powder.

The gel precursors was calcined at 400°C and 800°C for 5 hours in a muffle furnace. X-ray powder diffraction was used to study the crystallinity of the prepared powder with respect to annealing temperature. Purity of sample was determined using FT-IR. The intercalation and deintercalation properties of the cathode material was analysed using cyclic voltammeter.

### 3.2 Fourier Transform Infrared Spectroscopy (FT-IR)

Fourier transform infrared spectroscopy (FT-IR), is the most advanced method of infrared spectroscopy. The basic component of FT-IR Spectrometer is the Interferometer. The most widely used interferometer is the Michelson Interferometer. A simple scheme of Michelson Interferometer is shown in figure 3.2 (Pachler et al, 1998)

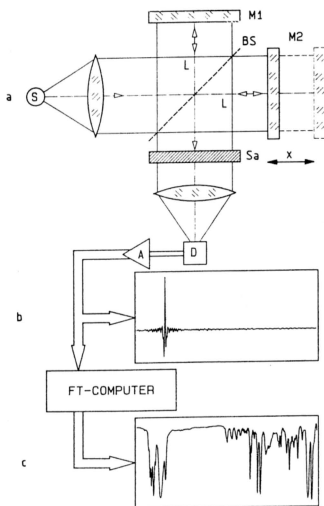


Figure 3.2 : Scheme of a Michelson Interferometer - S radiation source, As sample cell, D detector, A amplifier, M1 fixed mirror, M2 moving mirror, BS beam splitter

The infrared spectra originates primarily from the vibration, stretching and bending modes within molecules, as shown in figure 3.3 . Most organic and inorganic materials shows absorption of infrared radiation.

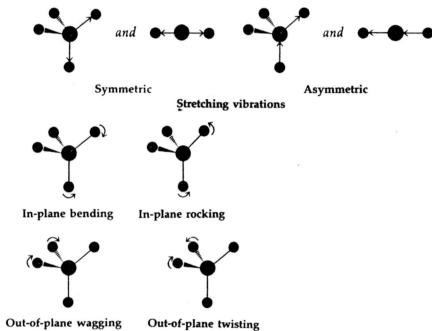


Figure 3.3 : Some stretching and bending vibrations of polyatomic molecules  
( Pine , 1987)

Infrared spectroscopy is mainly used for identification of substances or the determination of structures. Infrared spectra can reveal both the specific functional groups present and their general location in a molecule (Harris and Kratochvil, 1982)

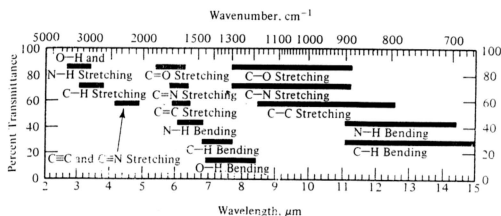


Figure 3.4 : Correlation of groups vibrations with general regions of infrared absorption ( Fritz and Schenk, 1979)

### 3.3 X-ray diffraction

In 1912, von Laue discovered diffraction of X-rays by crystals and explained the observed diffraction patterns in terms of a theory analogous to that used to treat diffraction by gratings, extended to three dimensions. On the other hand, Bragg interpreted it in terms of reflection from planes through the points in crystal lattice. This term "reflection" is analogous to that from a mirror, for which angle of incidence is equal to angle of reflection. Waves scattered from adjacent lattice planes will be just in phase only for certain angles of scattering, as shown in figure 3.5 (Glusker and Trueblood, 1985).

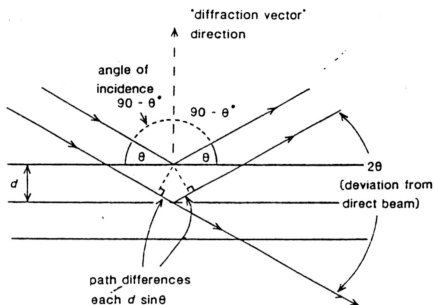


Figure 3.5 : Bragg equation (Glusker and Trueblood, 1985).

From such considerations Bragg derived the famous equation

$$n\lambda = 2d \sin \theta$$

- $\lambda$  = wavelength of radiation
- $n$  = an integer
- $d$  = perpendicular spacing between lattice planes
- $\theta$  = angle of incidence

The two treatments of X-ray diffraction are equivalent. The approach by von Laue provides more insight into the process of structural analysis by diffraction methods.

X-ray diffraction has provided a wealth of important information to science and industry. The arrangement and spacing of atoms in crystalline materials can be directly deduced from diffraction studies. X-ray diffraction is currently of importance in elucidating the structures of complex natural products as steroid,

vitamin and antibiotics (Skoog and West, 1980). Figure 3.6 shows an X-ray diffractometer.

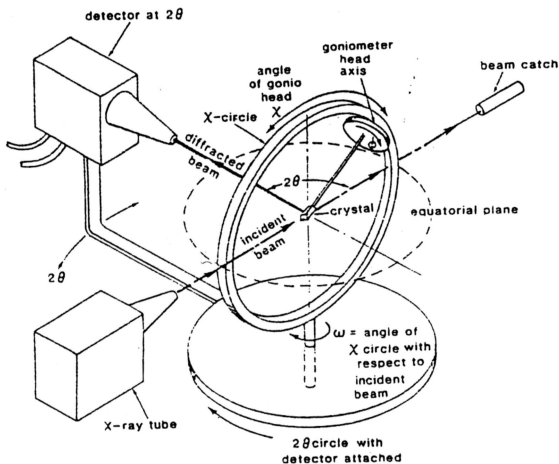


Figure 3.6: Diffractometry (Glusker and Trueblood, 1985)

X-ray diffraction provides a convenient and practical means for identification of crystalline compounds because each crystalline material has its own characteristic pattern. A compound can be identified from its powder diffraction pattern based upon the position of lines and their relative intensities. By comparing the spacing of



four most intense line of the unknown substance with d values for pure compounds from X-ray powder data file, it is possible identify the compound. A typical card is shown in figure 3.7 (Willard et al, 1981). In addition, X-ray diffraction pattern can give quantitative information concerning a crystalline compound in a mixture by measuring the intensity of lines and comparing with standards.

5-062B

d	2.82	1.99	1.63	1.258	NaCl		
I/I <sub>1</sub>	100	55	15	13	SODIUM CHLORIDE		
					HALITE		
Rad. Cu	λ 1.5405	Filter	Dia.		dÅ	I/I <sub>1</sub>	hkl
Cut off	1/I <sub>1</sub>						
Ref. Swanson and Fayat, NBS Circular 539, Vol. 11, 41 (1953)					3.258	13	111
					2.821	100	200
					1.994	55	220
					1.701	2	311
					1.628	15	222
					1.410	6	400
					1.294	1	331
					1.261	11	420
					1.1515	7	422
					1.0855	1	511
					0.9949	2	440
					.9533	1	531
					.9401	3	600
					.8917	4	620
					.8601	1	533
					.8503	3	622
					.8141	2	444
Sps. Cubic							
a <sub>0</sub> 5.6402	b <sub>0</sub>	c <sub>0</sub>	S.G. O <sub>h</sub> <sup>5</sup> - Fm3m				
α	β	γ	A	C			
Ref. Ibid.	Z 4 D <sub>2</sub> 2.164						
Ea							
2V	nωβ 1.542	εγ	Sign				
Ref. Ibid.	D	mp	Color				
An ACS reagent grade sample recrystallized twice from hydrochloric acid.							
X-ray pattern at 26°C.							
Replaces 1-0993, 1-0994, 2-0818							

Figure 3.7 : X-ray data card for NaCl (Willard et al, 1981).

AS10344648

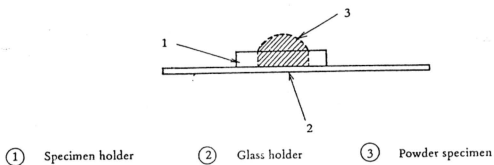


Figure 3.8 : Specimen Preparation ( Shidmadzu Instruction Manual)

The specimen sample was prepared by placing a little ground sample on a glass slide and mixed with acetone. By using the end of the spatula, the mixture was spread to obtain a thin uniform layer. The prepared specimen was analysed using a Shimadzu XD-5 diffractometer available at Geology Department of University Malaya using  $\text{Cu-K}_\alpha$  radiation. The diffraction pattern were taken at room temperature in the range of  $3^\circ < \theta < 70^\circ$  using step scans. X-ray diffraction patterns for  $\text{LiNi}_{1-y}\text{Co}_y\text{O}_2$  are shown in figure 3.9 (Zhecheva and Stoyanova, 1993).

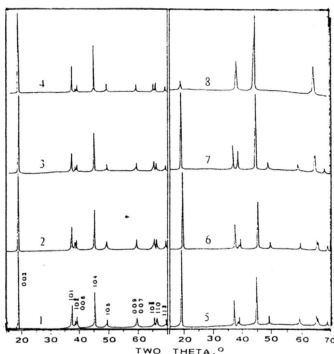


Figure 3.9 : XRD patterns of  $\text{Li}_x(\text{Co}_{1-y}\text{Ni}_y)_{2-x}\text{O}_2$  solid solutions obtained at  $850^\circ\text{C}$  . Sample notation : 1  $y = 0$ ; 2  $y = 0.1$ ; 3  $y = 0.2$ ; 4  $y = 0.4$ ; 5  $y = 0.6$ ; 6  $y = 0.8$ ; 7  $y = 0.9$  and 8  $y = 1$  (Zhecheva and Stoyanova, 1993).

### 3.4 Cyclic Voltammetry

Cyclic voltammetry is perhaps one of the more versatile analytical technique available to the electrochemist. The technique allows identification of reversible couples, study mechanisms and rates of oxidation-reduction processes and provide a tool to help unravel complex electrochemical systems. Essentially the technique applies a linearly changing voltage to an electrode (Broadhead and Kuo, 1994).

A redox couple in which both species rapidly exchange electrons with the working electrode is termed an electrochemically reversible couple (Heinemann and Kissinger, 1996). By measuring potential difference between two peak potentials from a cyclic voltammogram, such a couple can be identified.

$$\Delta E_p = E_p^A - E_p^C$$

$$E_p^A = \text{Anodic peak potential}$$

$$E_p^C = \text{Cathodic peak potential}$$

A reversible reaction will have a peak current  $I_p$  that is proportional to the square root of the scan rate which is known as the Randles-Sevcik equation:

$$I_p = -0.4463nF(nF/RT)^{1/2} \cdot (D\nu)^{1/2} \cdot C_o^\infty$$

Where

$n$  = number of electrons which is transferred in the electron transfer step.

$F$  = Faraday's constant  $96500/C \text{ mol}^{-1}$

$R$  = gas constant  $8.3142/J \text{ mol}^{-1} \text{ K}^{-1}$

$D$  = diffusion constant  $m^2 s^{-1}$

$\nu$  = scan rate  $V s^{-1}$

$C_o^\infty$  = electroactive species concentration in solution

Other information that can be studied whether the electrochemical reaction is reversible or otherwise is given below (Basirun, 2000):

For a reversible electrochemical reaction:

1.  $\Delta E_p = E_p^A - E_p^C = (59/n)/\text{mV}$  at 2908K
2.  $|E_p - E_{p/2}| = (59/n)/\text{mV}$  at 298K
3.  $|I_p^A/I_p^C| = 1$
4.  $I_p$  proportional to  $v^{1/2}/(Vs^{-1})^{1/2}$
5.  $E_p$  independent of  $v/Vs^{-1}$

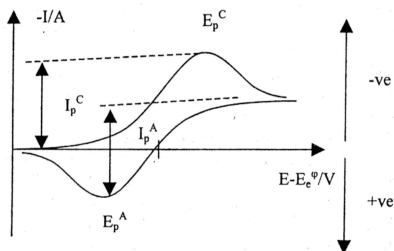


Figure 3.10: Cyclic voltammetry for a reversible process. Only species O present in solution  $O + e \rightarrow R$  (Basirun, 2000).

The cyclic voltammetric studies was performed using Electrochemical Analyzer BAS100B instrument. The working electrode was prepared by mixing 90% sample with 10% PVDF and the mixture was placed in a glass tube. The material was compressed with a glass rod and a fine copper wire was attached to the material as shown in figure 3.11. The diameter of electrode was 3mm.

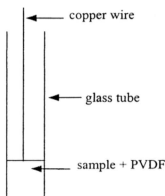


Figure 3.11: Working electrode

Carbon was used as the counter electrode and Ag/AgCl as the reference electrode. The electrolyte was prepared by dissolving 1M  $\text{LiSO}_3\text{CF}_3$  in 50 : 50 (v/v) mixture of dimethyl carbonate (DMC) / propylene carbonate. The prepared electrolyte (100  $\text{cm}^3$ ) was deoxygenated by bubbling nitrogen gas. The prepared working electrode was transferred to cell and cycling was carried out at different scan rates.

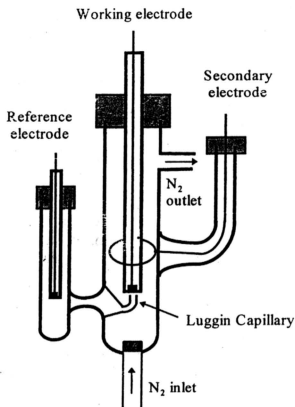


Figure 3.12 : The electrochemical cell (Arof et al, 2000)

### 3.5 Battery Fabrication

Besides, cyclic voltammetry, there are many different electroanalytical techniques available to determine electrochemical parameters and evaluating couples as candidates for new batteries. One of them is chronopotentiometry, which involves the study of voltage at an electrode upon which is imposed a constant current. It is sometimes known as galvanostatic voltammetry. In this technique a constant current is applied to an electrode, and its voltage response indicates the changes in electrode process occurring at its interface (Broadhead and Kuo, 1994).

To describe the principles behind galvanostatic voltammetry, consider the following reaction given in the equation below, where species O is reduced.



When a constant current is passed through the system, the concentration of O in the vicinity in the electrode surface will begin to decrease. As a result of this depletion, O diffuses from the bulk solution into the depleted layer. As the electrode process continues, eventually the surface concentration of O falls to zero. The electrode can no longer support the electroreduction of O. Therefore, an additional cathodic reaction must be brought into play and an abrupt change in potential occurs. Figure 3.13 shows potential time relationship for a reversible reduction electroactive species.

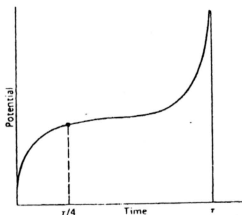


Figure 3.13: Potential curve at constant current for reversible reduction of an electroactive species (Broadhead and Kuo, 1994).



When a cell or battery is discharged, its voltage is lower than the theoretical voltage. The difference is caused by IR losses due to cell resistance and polarisation of active materials during discharge (Broadhead and Kuo, 1994). This is shown in figure 3.14. Ideally one should have a discharge curve similar to curve 1, where the potential is almost constant throughout discharge and falls fairly sharp to zero when the voltage of the battery falls below its working voltage. Curve 2 is similar to curve 1, but represents a cell with a higher internal resistance or higher discharge rate

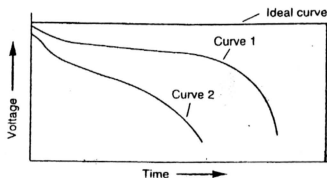


Figure 3.14 : Characteristic discharge curves (Broadhead and Kuo, 1994).

Important parameters of a cell can be obtained from a charge/discharge curves. By knowing the transition time, mass of the cell, the parameters of discharge capacity, power and energy densities can be calculated.

Charge/discharge studies were carried out on  $\text{LiNiO}_2$  calcined at  $800^\circ\text{C}$  for 14 hours in order to test its suitability as cathode-active materials in high voltage containing batteries. The test cell was fabricated using  $\text{LiNiO}_2$  cathode, carbon anode and a non-aqueous  $\text{Li}^+$  ion conducting organic electrolyte. The electrochemical cell was fabricated as follows. The composite cathode consists of  $\text{LiNiO}_2$  powder, carbon,

DBP and PVDF binder in the 74:13:3:10 weight ratio. Acetone was added to the mixture and stirred with a magnetic stirrer to form a homogenous mixture. The mixture was heated at 50°C until most of the acetone had evaporated. The resulting slurry was spread on a petri dish to form an electrode film. A 3cm x 5cm square film was cut and pressed on to an aluminium mesh by applying pressure. The cathode was dried at 150°C in air. A similar procedure was used, to prepare the carbaceous anode. Carbon, DBP and PVDF in the ratio of 80: 10: 10 was used. A copper mesh was used instead of aluminium. The electrolyte solution was a mixture of PVC- PEO- LiCF<sub>3</sub>SO-DBP: DMC in the ratio 70 : 30. The cell was assembled using a cell holder made up of Teflon. The typical cell diagram is shown in figure 3.15 (Jacob et al, 2000). A computer controlled galvanostat (BAS LG 50) was employed to acquire the charge /discharge data on the assembled cell.

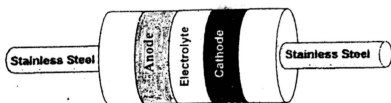


Figure 3.15 : Cell assembly (Jacob et al , 2000).